International Forum on Aeroelasticity and Structural Dynamics
IFASD 2015
June 28 — July 02, 2015 ▲ Saint Petersburg, Russia

FREQUENCY-DOMAIN APPROACH FOR TRANSONIC UNSTEADY AERODYNAMICS MODELLING

Adrien Poncet-Montanges[1], D. Jones[2], A.L. Gaitonde[3], J. E. Cooper[4], Y. Lemmens[5]

[1] Dept of Aerospace Engineering, University of Bristol, UK.
adrien.poncet-montanges@bristol.ac.uk

[2] Dept of Aerospace Engineering, University of Bristol, UK.
dorian.jones@bristol.ac.uk

[3] Dept of Aerospace Engineering, University of Bristol, UK.
ann.gaitonde@bristol.ac.uk

[4] Dept of Aerospace Engineering, University of Bristol, UK.
J.E.Cooper@bristol.ac.uk

[5] Siemens Industry Software NV, Belgium.
yves.lemmens@siemens.com

Keywords: reduced order models, unsteady aerodynamics, frequency domain, IFASD.

Abstract: As part of the ALPES (Aircraft Loads Prediction using Enhanced Simulation) project, this paper presents a way of building a reduced order model by using the Eigenvalue Realization Algorithm in the frequency domain, and applies it to model the aerodynamic response of a pitching airfoil in the transonic domain. With input data obtained with the TAU linearized frequency domain solver for a NLR7301 airfoil, the reduced order model shows a strong ability to reconstruct the frequency response.

1 INTRODUCTION

Computational Fluid Dynamics (CFD) has now a wide range of validity where it gives highly accurate results with regards to wind tunnel experiments. It is extensively used in the industry for steady analysis such as performance studies. However, unsteady aerodynamics has to be used for aircraft design and aeroelastic applications such as flutter speed or limit cycle oscillation prediction. More powerful computers have enabled the application of CFD for unsteady loads calculations, but the computational cost remains high, especially when it comes to viscous flows.

System identification consists on building a mathematical description of the dynamic behavior of a system from measured data. The model aims at providing accurate prediction of the system comportment for a given input ([1], [2], [3], [4] [5]). Whereas real systems are often costly to describe, models can capture their essential behavior. The modelling approach, so called inverse problem [6], consists on determining causes from knowing the effects. This is to opposite of a direct problem. As same effects can have different causes, inverse problems may have different solutions. Contrary to direct problems, there is not only one way of solving them; but a few methods are generally applicable. These inverse problems can be linear (system of equations or integral equation) or non-linear.

It then becomes obvious that models are useful and can be used to explain data, understand phenomena and predict behaviors. For many of them, a high number of degrees of freedom leads to extended calculation times. Then, reduced order models (ROM) aim at decreasing the CPU time by keeping a few degrees of freedom of the numerical model. They nevertheless succeed in keeping good accuracy and stability. These ROMs enable [7] to simplify the study of the system, and to get command laws more easily. Model order reduction can be achieved using different methods; these depend on the physics of the system, the accuracy wanted and the information availability. The latest can be based on physical equations, engineering problems, datasets and so on. For systems whose model is strongly linked to the physics, order reduction can even be performed by hand, thinking about the independencies between the parameters; interpolation can also be used.

While building a ROM, a first technique is to define projection bases and spaces. The idea is the use linear algebra and to construct a subspace orthogonal to the Krylov subspace; this can be performed thanks to the Gram-Schmidt orthonormalization method. Since it can be unstable [8] or a modified Gram-Schmidt can be used. In order to achieve this, Arnoldi developed an iterative algorithm [9]. If the system matrix is hermitian, the Lanczos method [10] is much faster. It is based on the Arnoldi method, but as the system matrix is symmetric, the algorithm is much simpler and the recurrence is shorter: each vector U_{j+1} is directly calculated from the two previous ones U_j and U_{j-1}. The Lanczos algorithm can also be combined with a Padé approximation, for a method called Padé via Lanczos (PVL). This method aims to preserve the stability of the system. In fact, the reduced order modeling techniques using the Padé approximation do not enable to carry this stability [11]. Other methods such as partial PVL [12] enable to correct the poles and the zeros of the reduced transfer function; it leads to an enhanced stability. Antoulas [13] uses the advantages of both Krylov subspaces and balanced truncation approaches. Finally, the Passive Reduced-order Interconnect Macromodelling Algorithm, while using the Arnoldi method guarantees the preservation of passivity and enables an enhanced accuracy [14].

Another stream of scientific analysis uses the system response of different excitations to identify the reduced matrices. Based on Hankel singular values, several algorithms were developed for model reduction such as singular value decomposition (SVD). The idea is to eliminate the states requiring a large amount of energy to be reached, or a large amount of energy to be observed, as both correspond to small eigenvalues [15]. Gramians are introduced since they can be used to quantify these amounts of energy. The reachability gramian quantifies the energy needed to bring a state to a chosen value, whereas the observability gramian quantifies the energy provided by an observed state [16]. The value of these gramians obviously depends on the basis on which they are calculated. In the case of a stable system, it exists a basis in the state space in which states that are difficult to reach are also difficult to observe. Normally, the Hankel singular values decrease rapidly. The balanced truncation aims at truncating the modes that are not both reachable and observable. They correspond to the smallest Hankel singular values. The singular value decomposition is well-conditioned, stable and can always work, but can be expensive to compute. It implies to solve high-dimensional Lyapunov equations [17] ; the storage required is of the order $O(n^2)$, while the number of operations is of the order $O(n^3)$. Many balancing methods exist, such as stochastic balancing, bounded real balancing, positive real balancing [18]. The frequency weighted balancing [19], can be useful if a good approximation is needed only in a specific frequency range. However, the reduced model is not necessarily stable if both input and output are weighted. These frequency weighted balancing methods have undertaken many improvements: the most recent one guarantees stability and yields to a simple error bound [20]. Based on Markov parameters, the Padé approximation (moment matching method) [21] has then been improved by Arnoldi and Lanczos [10] and is particularly recommended in the case of high dimension systems.

In this paper the algorithm chosen is the Eigensystem Realization Algorithm [22], using the singular value decomposition of the Hankel matrix whose coefficients are the Markov parameters. The method proposed enables to build a model based on experimental data without knowing the system matrix. It is adapted for an input being given in the discrete frequency domain and uses a bilinear transformation to switch to the continuous space. A singular value decomposition is then performed to keep the dominant modes of the frequency response.

For given flow conditions, the frequency response of the integrated aerodynamic coefficients is directly related to the frequency of the pitching motion. Hence, it is relevant to build a reduced order model of the frequency response in the frequency domain instead of performing a classical reduction in the time domain. After solving the system and transforming back in the continuous space, it is possible to reconstruct any motion in the time domain. The method is applied to a pitching airfoil in subsonic and transonic range, with no shock-induced separation.

2 PROBLEM FORMULATION

2.1 MIMO in discrete and continuous spaces

A discrete-time linear and stable MIMO model of n-th order, with r-input and m-output can be described using the following state space representation

$$\begin{aligned} \dot{\boldsymbol{x}(t)} &= \hat{A}\boldsymbol{x}(t) + \hat{B}\boldsymbol{u}(t) \\ \boldsymbol{y}(t) &= \hat{C}\boldsymbol{x}(t) + \hat{D}\boldsymbol{u}(t) \end{aligned} \tag{1}$$

$\boldsymbol{x}(t) \in \mathbb{R}^{\mathrm{n}}$ represents the vector of different degrees of freedom (called state vector in control theory). It contains for example the unknown physical variables, such as velocity, pressure, density. $\boldsymbol{y}(t) \in \mathbb{R}^{\mathrm{p}}$ and $\boldsymbol{u}(t) \in \mathbb{R}^{\mathrm{m}}$ respectively represent the vector of the outputs of interest of the system, and the vector of inputs. Another convenient notation is also used for a discrete-time model:

$$\sum = \begin{pmatrix} \hat{A} & \hat{B} \\ \hat{C} & \hat{D} \end{pmatrix} \tag{2}$$

As far as a continuous-time is concerned, the matrices are written in this paper under the form

$$\sum = \begin{pmatrix} A & B \\ C & D \end{pmatrix} \tag{3}$$

Let the frequency response be given uniformly spaced between 0 and π, i.e. it is possible to provide the impulse response coefficients G_k for the N discrete frequencies

$$\widehat{\omega}_k = \frac{k\,\pi}{N}, \mathrm{k} \in [0\,,\mathrm{N}] \tag{4}$$

These discrete frequencies can be transformed to equivalent continuous frequencies using the Bi-Linear transform.

$$\omega_k = \frac{2}{T} \tan \frac{\widehat{\omega}_k}{2} \tag{5}$$

This bijective function transforms a discrete frequency $\widehat{\omega}_k \in [0, \pi]$ in a continuous frequency $\omega_k \in [0, \infty]$. The bilinear transformation has multiple advantages: it keeps the controllability and the observability properties from discrete to continuous [23], and from continuous to discrete. There is then an equivalence in the stability of system described in discrete and continuous space, assuming that this system is asymptotically stable.

2.2 Singular Value Decomposition

To map the whole unit circle, the algorithm extends the domain of the input data to the interval $]\pi, 2\pi]$ using the conjugate of G_k:

$$G_{k+N} = \overline{G_{N-k}} \tag{6}$$

The aim is then to perform a singular value decomposition of the Hankel matrix defined using the 2N-points inverse discrete Fourier transform (IDFT). The coefficients of the IDFT are defined such as

$$\widehat{h}_i = \frac{1}{2N} \sum_{k=0}^{2N-1} G_k \, e^{i2\pi j\omega k/2N} \quad , i \in [0, 2N-1] \tag{7}$$

and enable to build the block Hankel matrix, i.e. a square block of with constant elements across the anti-diagonals

$$\widehat{H} = \begin{pmatrix} \widehat{h}_1 & \widehat{h}_2 & \cdots & \widehat{h}_r \\ \widehat{h}_2 & \widehat{h}_3 & \cdots & \widehat{h}_{r+1} \\ \vdots & \vdots & \ddots & \vdots \\ \widehat{h}_m & \widehat{h}_{m+1} & \cdots & \widehat{h}_{m+r-1} \end{pmatrix} \text{with } m > n, r \geq n \text{ and } m + r \leq 2N \tag{8}$$

As the Hankel block matrix is real, according to the SVD theory [24], it exists $\widehat{U}$, $\widehat{\Sigma}$ and $\widehat{V}$ such as:

$$\widehat{H} = \widehat{U} \, \widehat{\Sigma} \, \widehat{V}^T \tag{9}$$

The model reduction is obviously performed by keeping the largest singular values. This is done by separating $\widehat{U}$ in $\widehat{U_s}$ and $\widehat{U}_o$ such as

$$\widehat{H} = [\, \widehat{U}_s \, \widehat{U}_o] \begin{bmatrix} \widehat{\Sigma}_s & 0 \\ 0 & \widehat{\Sigma}_o \end{bmatrix} \begin{bmatrix} \widehat{V}^T \\ \widehat{V}_o^T \end{bmatrix} \tag{10}$$

The diagonal block matrix $\widehat{\Sigma}_s$ *c*ontains the r highest singular value, r being the chosen size of the reduced order model.

2.3 Calculation of discrete reduced A and C

Once $\widehat{U}_s$ has been built by truncation of $\widehat{U}$, computing the discrete and reduced matrices $\hat{A}_r$ and $\hat{C}_r$ is achieved with [25]:

$$\hat{A}_r = \frac{\left(J_1\,\widehat{U}_s\right)^*\left(J_1\,\widehat{U}_s\right)}{\left(J_1\,\widehat{U}_s\right)^*\left(J_2\,\widehat{U}_s\right)} \tag{11}$$

$$\hat{C}_r = \left(J_3\,\widehat{U}_s\right) \tag{12}$$

where

$$\begin{aligned} J_1 &= \left[I_{(m-1)p}\ 0_{(m-1)p*p}\right] \\ J_2 &= \left[0_{(m-1)p*p}\ I_{(m-1)p}\right] \\ J_3 &= \left[I_p\ 0_{p*(m-1)p}\right] \end{aligned} \tag{13}$$

2.4 Calculation of discrete reduced B and D

Since the state-space model G can be written as

$$G = C(zI - \hat{A}_r)^{-1}B + D, z \in \mathbb{C}, \tag{14}$$

For N ≥ n, then Ω is defined such as

$$\Omega = \begin{bmatrix} \hat{C}_r(z_0 I - \hat{A}_r)^{-1} & I_p \\ \hat{C}_r(z_1 I - \hat{A}_r)^{-1} & I_p \\ \vdots & \vdots \\ \hat{C}_r(z_N I - \hat{A}_r)^{-1} & I_p \end{bmatrix} \in \mathbb{R}^{(N+1)p*(n+p)},\ \forall \mathrm{k} \in [0\ ,\ \mathrm{N}],\ z_k = e^{j\omega_k t} \tag{15}$$

So (14) can be written as

$$\Omega \begin{bmatrix} \widehat{B} \\ \widehat{D} \end{bmatrix} = G \tag{16}$$

Let $\breve{\Omega}$ be composed of the real and imaginary parts of Ω.

$$\breve{\Omega} = \begin{bmatrix} Re(\Omega) \\ Im(\Omega) \end{bmatrix} \tag{17}$$

$\widehat{B}_r \in \mathbb{R}^{r,1}$ and $\widehat{D}_r \in \mathbb{R}$ can are calculated by

$$\begin{bmatrix} \widehat{B}_r \\ \widehat{D}_r \end{bmatrix} = \breve{\Omega}\,\breve{\Omega}^T \left(\breve{\Omega}^T\ \begin{bmatrix} Re(G) \\ Im(G) \end{bmatrix}\right)^{-1} \tag{18}$$

2.5 Bilinear transformation

The continuous-time system G defined as

$$G(z) = D_r + C_r(zI - A_r)^{-1}B_r \tag{19}$$

can be transformed in a discrete-time system

$$\hat{G}(z) = \widehat{D_r} + \widehat{C_r}(zI - \hat{A}_r)^{-1}\hat{B}_r \tag{20}$$

using the bilinear transformation [26]:

$$A_r = \frac{2}{T}\,(I_r + \hat{A}_r)^{-1}\,(I_r - \hat{A}_r) \tag{21}$$

$$B_r = \frac{2}{\sqrt{T}}(I_r + \hat{A}_r)^{-1}\,\hat{B}_r \tag{22}$$

$$C_r = \frac{2}{\sqrt{T}}\,\hat{C}_r\,(I_r + \hat{A}_r)^{-1} \tag{23}$$

$$D_r = \hat{D}_r - \hat{C}_r\,(I_r + \hat{A}_r)^{-1}\,\hat{B}_r \tag{24}$$

2.6 Comparison between the sample data and the model built

The model can be used to reconstruct the frequency response G_r on a chosen number N_r of equispaced discrete frequencies corresponding to the same number of continuous frequencies.

$$G_k(z) = D_r + C_r(\omega_k\,I_r - A_r)^{-1}\,B_r, \qquad \forall k \in [0\,, N] \tag{25}$$

3 APPLICATION TO THE MODELLING OF A PITCHING AIRFOIL

3.1 Numerical model

The aim is to model of the aerodynamic behavior of an airfoil in a pitching motion at different frequencies. The motion is sinusoidal and described by the following equation:

$$\alpha = \alpha_m + \alpha_0 \cdot \sin\,(\omega \cdot t\,) \tag{26}$$

where α_m is the mean angle of attack, α_0 the amplitude and ω the frequency of the motion.

Let U_∞ be the freestream velocity and c the airfoil chord, the reduced frequency is defined such as

$$k = \frac{\omega \cdot \mathrm{c}}{U_\infty} \tag{27}$$

The order of magnitude of the range of reduced frequencies used in unsteady aerodynamic is between 10^{-2} and 10. The airfoil chosen is a NLR7301 since it is supercritical; then it is close to the profiles used in aircraft design. Moreover, the literature provides many results for validation. To be able to use CFD, two different meshes are created for viscous and inviscid simulations with TAU [27].

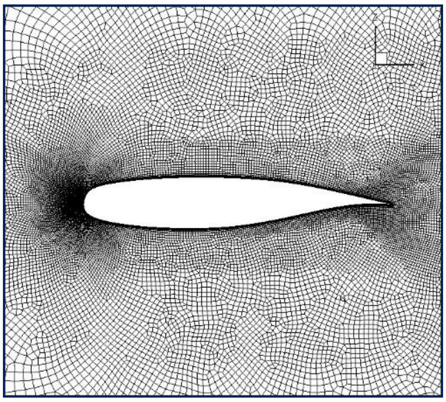

Figure 1: Viscous mesh, NLR 7301

As far as the turbulence is concerned, Spalart-Allmaras [28] is selected as it combines good accuracy and robustness. The RANS equations are discretized in a central way, with a scalar dissipation scheme. Finally, the chosen relaxation solver is Backward Euler.

The convergence is reached for every calculation performed in the following part. A far as unsteady RANS simulations are concerned, the behavior is checked by maintaining a value of y_+ below 1. The numerical model has been validated after several comparisons to wind tunnel data [29]. for steady, quasi-steady and unsteady computations.

The pressure coefficient is given by

$$C_p = \frac{p - p_\infty}{\frac{1}{2}\ \rho_\infty V_\infty^2} \tag{28}$$

When calculated at multiple points around the airfoil, it enables to plot the pressure distribution in subsonic and transonic cases (Mach=0.5 and Mach=0.68). The shock position is clearly visible for x/c=0.2.

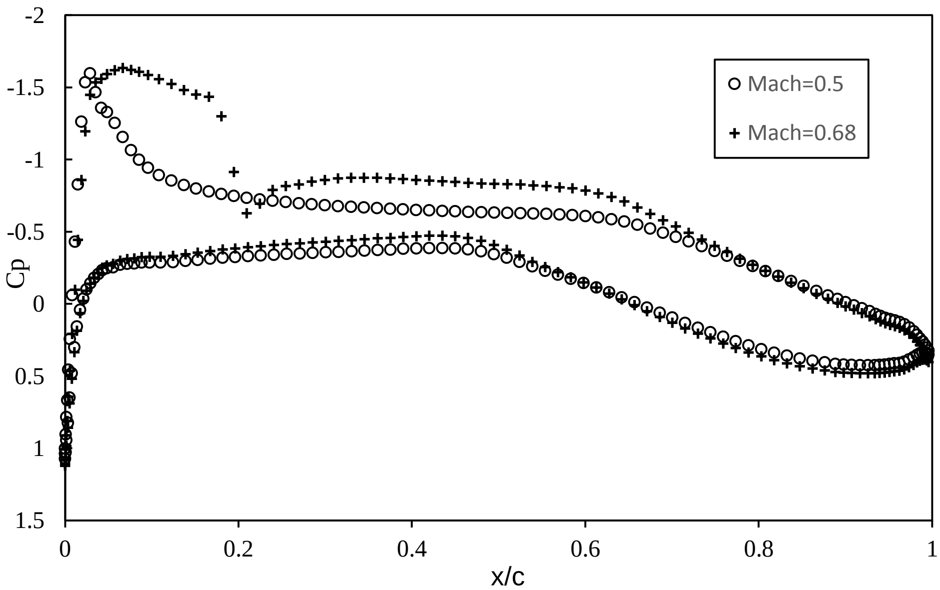

Figure 2: Cp distribution, steady Euler, α=0.5°

3.2 Linearized frequency domain solver

3.2.1 Basics

In addition to the classical unsteady RANS and Euler computations, as the amplitude of the motion is small and the motion periodic, it is possible to use the linearized frequency domain solver [30].

An unsteady governing equation of the fluid motion discretized in space can be written

$$\frac{d\boldsymbol{u}}{dt} + R(\boldsymbol{u}, \boldsymbol{x}, \dot{\boldsymbol{x}}) = 0 \tag{29}$$

where R is the residual, written as a function of the flow solution u, the grid coordinates x and the grid velocities $\dot{x}$. Under the assumption of a small amplitude of the unsteady perturbations, the RANS equation can be linearized around the steady state, i.e. it is seen as the superposition of the steady state mean and of the perturbation.

$$\boldsymbol{u}(t) = \overline{\boldsymbol{u}} + \widetilde{\boldsymbol{u}}(t)\,, \qquad \|\widetilde{\boldsymbol{u}}\| \ll \|\overline{\boldsymbol{u}}\| \tag{30}$$

$$\boldsymbol{x}(t) = \overline{\boldsymbol{x}} + \widetilde{\boldsymbol{x}}(t), \qquad \|\widetilde{\boldsymbol{x}}\| \ll \|\overline{\boldsymbol{x}}\| \tag{31}$$

and transformed in the frequency domain, since the perturbation is assumed to be periodic and can expressed as

$$\tilde{x}_k(t) = \sum_k Re(\hat{x}_k\, e^{jk\omega t}) \tag{32}$$

where $\hat{x}_k$ are the complex Fourier coefficients of the motion, ω the frequency, k the mode and j complex number such as

$$j = \sqrt{-1} \tag{33}$$

After replacing the linearized values of u(t) and x(t) in (29), the following system is obtained

$$A\boldsymbol{x} = b \; where \; A = \begin{pmatrix} \frac{\partial R}{\partial u} & -\omega I \\ \omega I & \frac{\partial R}{\partial u} \end{pmatrix}, b = \begin{pmatrix} \frac{\partial R}{\partial x} & -\omega \frac{\partial R}{\partial \dot{x}} \\ \omega \frac{\partial R}{\partial \dot{x}} & \frac{\partial R}{\partial x} \end{pmatrix} \begin{pmatrix} \tilde{x}_{Re} \\ \tilde{x}_{Im} \end{pmatrix} \tag{34}$$

The Jacobian $\partial R / \partial u$ is theoretically calculated in TAU, but the right hand term is evaluated by using central finite differences [31].

3.2.2 Results

The model enables to give fast and accurate values for the magnitude and phase of the aerodynamic coefficients. The figure 3 shows the lift magnitude obtained in transonic domain (Mach=0.68, α_m=0.5, α_0=0.15) for different types of calculations at different reduced frequencies in the range of interest.

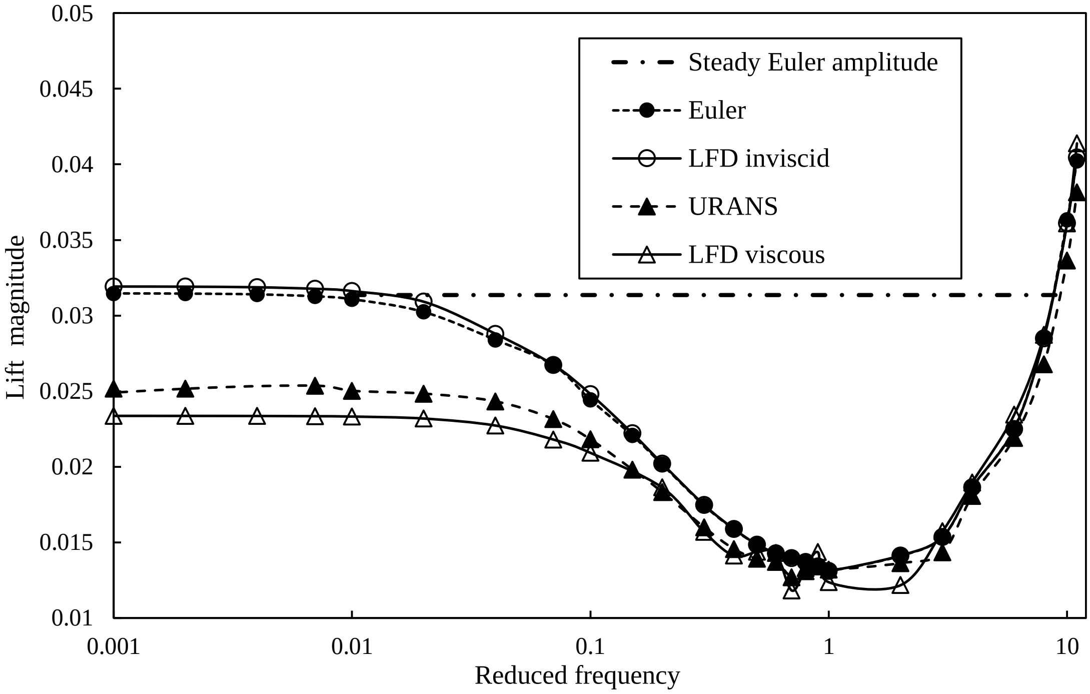

Figure 3: Viscous and inviscid validation of the LFD solver

The LFD solver is highly accurate, especially for inviscid computations, as soon as the amplitude of the pitching is small, which is the condition for the linearization ; it presents the advantage to be much faster than an unsteady Euler simulation (30 times faster in average, estimated on the calculation launched at the university of Bristol). It will then be used in the following part to provide the input to build the reduced order model.

3.3 Choice of T

As defined in (5), T is governing parameter of the bilinear transformation

$$\omega_c = \frac{2}{T}\tan\frac{\omega_d}{2} \tag{35}$$

According to the theory, ω_d has to be chosen equispaced between 0 and π. The choice of T is important as it has a major importance in the relationship between continuous and discrete frequencies. As it is easier to think in terms of reduced frequency, ω_d is transformed in k_d.

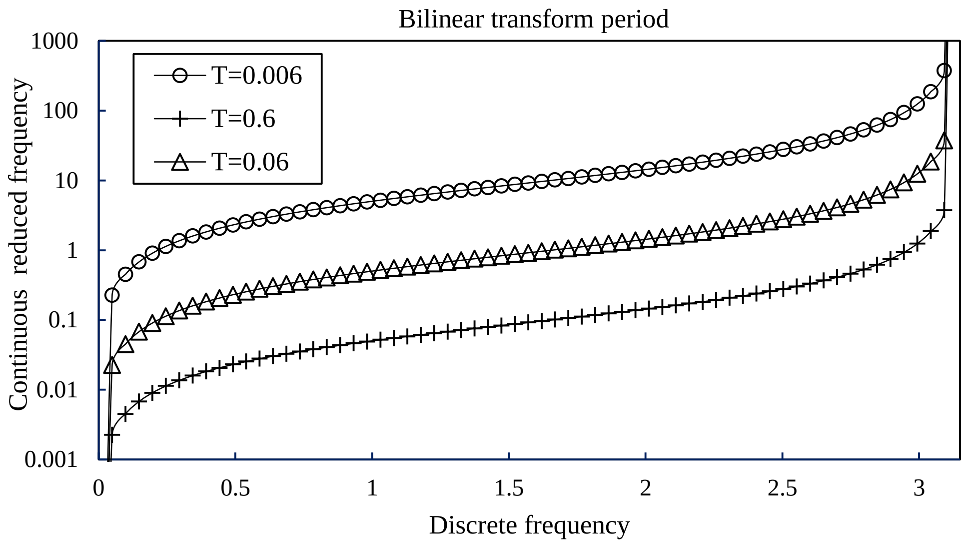

Figure 4: Choice of the sampling

T has to be chosen such as the continuous reduced frequencies are in the range of interest of the model input. T=0.006 provides continuous reduced frequencies mostly in the interval [1,100] (Figure 4), and the model will not be able to reconstruct accurately the magnitude and phase of the aerodynamic coefficient for low frequencies. The same remark can be applied for T=0.6, where the information will be poor at high frequencies. However, T=0.06 seems to be a good choice as the corresponding reduced frequencies cover well the aerodynamic range of interest.

3.4 Reduced order model

3.4.1 Input data

In order to assess the quality of the reduced order model, three values of T are chosen, and for each of those, 256 LFD calculations are launched. They enable to build ROMs of different sizes in a systematic way with a different number of input data. The error between the prediction of the model and the LFD calculation for both magnitude and phase of C_L and C_M is calculated and plotted. As the discrete frequencies are equispaced, it is straight forward to use a cross-validation. This technique enables to estimate the performance of the model depending of the number of training points and the size of the model built. N=256 being the number of training points, different models are created with $N/2i$ samples, i ∈ [2,4,8,16].

For each model, the quality is judged by reconstructing each magnitude and phase corresponding to the N frequencies of the training set and by comparing it to the LFD results. To represent the model performance, a root-mean-square error is calculated (Figure 5).

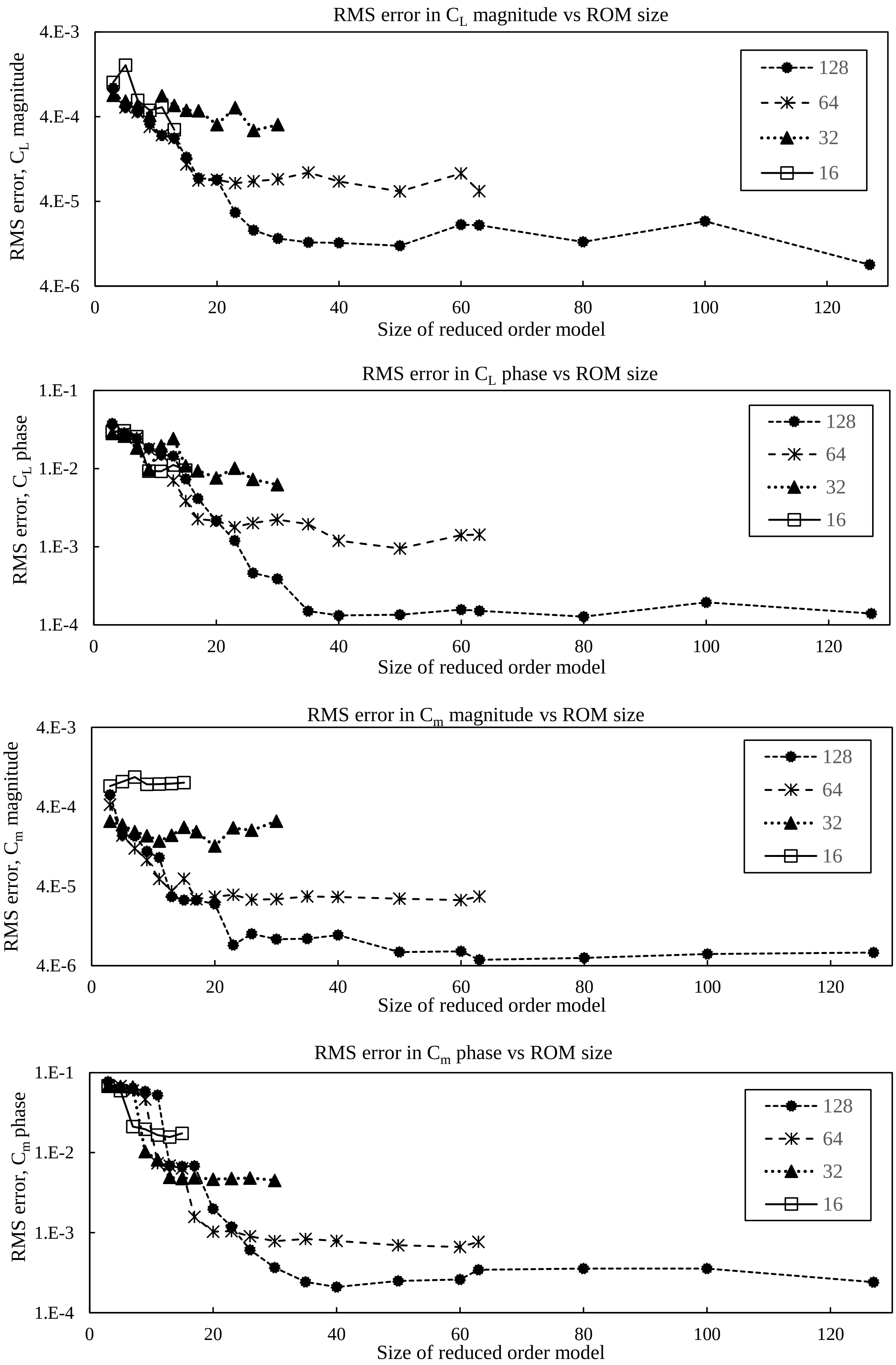

Figure 5: Root-mean-square error in lift and moment, T=0.06

For the different reduced order built, the RMS error appears has the same trend for the lift and for the pitching moment. The error becomes obviously smaller when increasing the number of input frequencies, but 64 input points seems highly satisfactory. Moreover, a ROM size of 20 or more guarantees a really good accuracy for both magnitude and phase.

The following plots show the frequency response reconstructed by two models of size 9 and 23, and has to be compared to the values obtained with the LFD solver.

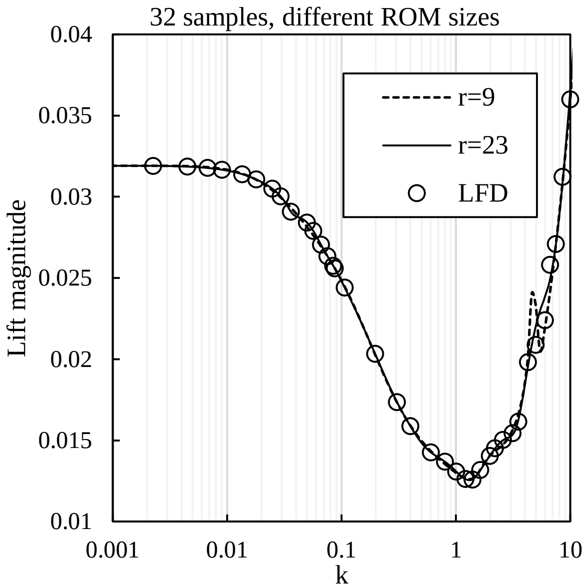

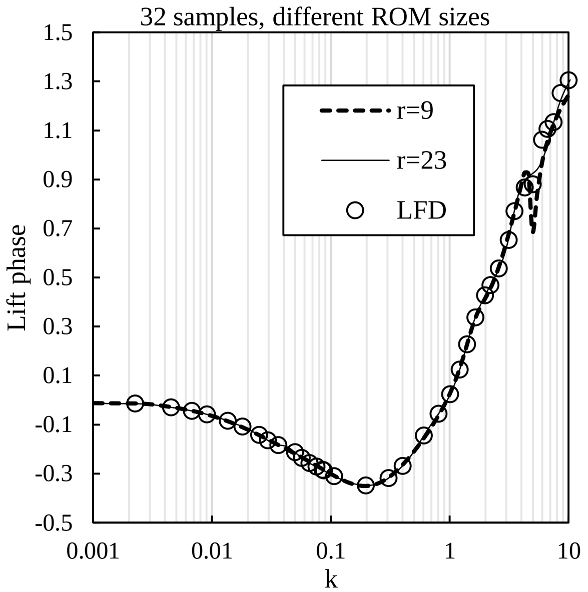

Figure 6: Comparison between the frequency responses of two different ROM, N=32, Mach=0.68

The small number of sample points leads to inaccuracies for k≈5 in magnitude and phase. Moreover, as far as the lift phase is concerned, the model experiences difficulties to reconstruct the low frequencies, due to a lack of input point in this region. However, the performance is already good in general.

With double the input points, the model gives the following frequency response

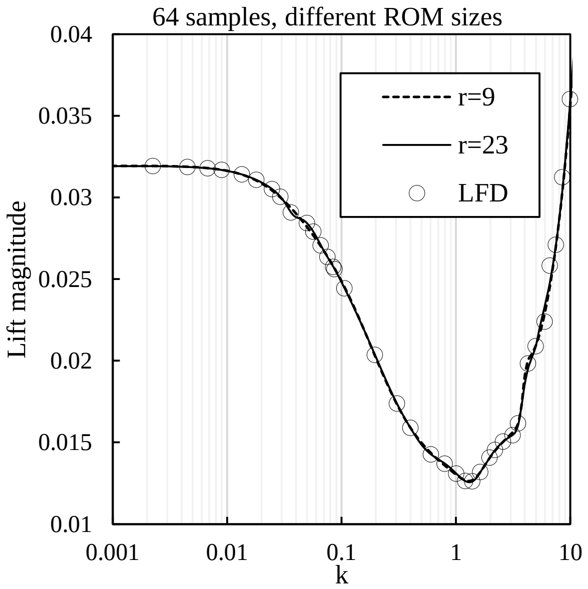

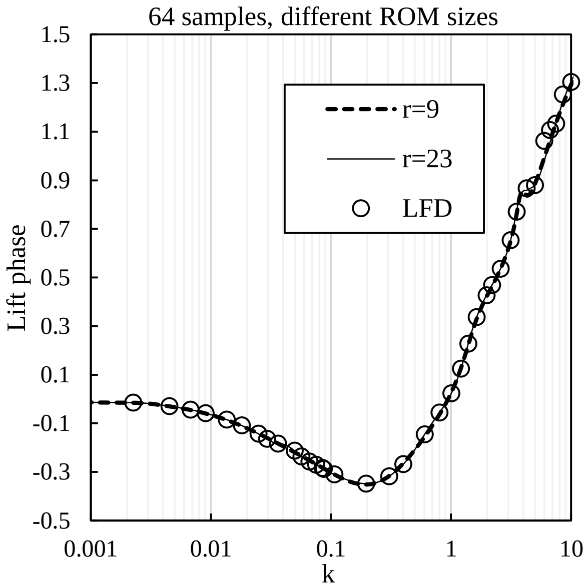

Figure 7: Comparison between the frequency responses of two different ROM, N=64

Even with a very small model (N_r=9), the error observed before for k≈5 as well as for the low frequencies has been corrected.

The advantage of this method is that it reconstructs the aerodynamic coefficients for any frequency between 0 and infinity. Therefore, for a given frequency, it is straight forward to reconstruct the aerodynamic coefficients during a period using the magnitude and the phase given as an output by the model. Two reduced order model of size Nr=3 and Nr=15 have been built with 32 samples, and the result is compared to the value given by a LFD calculation for the same frequency.

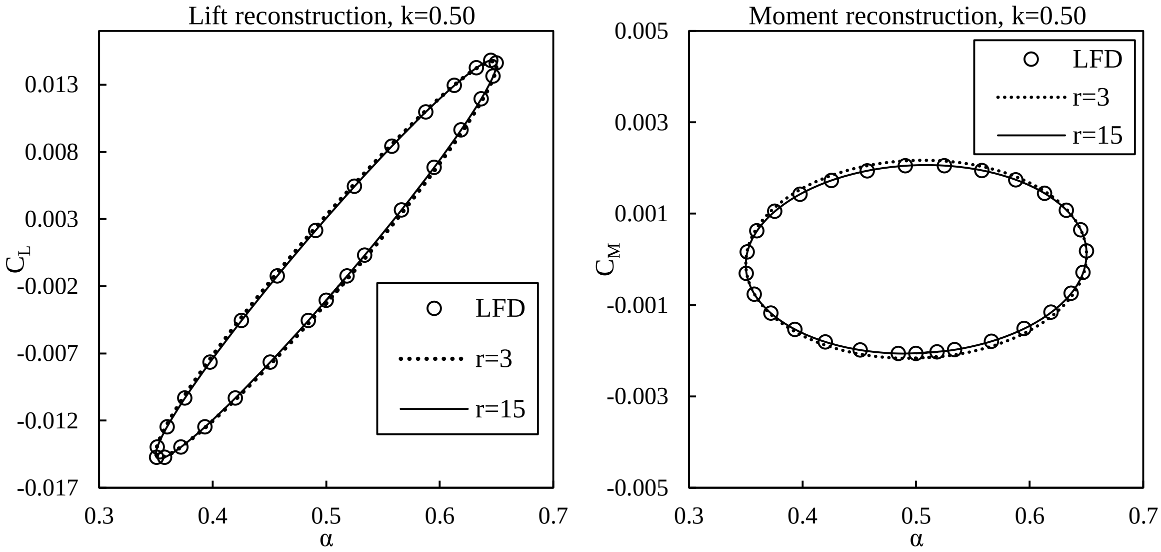

Figure 8: Lift and moment reconstruction, k=0.5, N=32, r=[3,5] vs LFD

As expected, since the error observed in figure 5 is small, the reconstructed lift and moment as a function of the angle of attack is really accurate when compared to the LFD reference, even if the model has been built with only 32 input frequencies.

4 CONCLUSIONS

A method has been presented to build a low order model in the frequency domain. It has been tested on aerodynamic results of a pitching airfoil and shows its ability to reconstruct the frequency response with a really good accuracy, even for very low orders and for a small number of sample points. As explained in this paper, T has however to be chosen carefully so that the input frequencies maps well the region of interest. Because of the equispaced nature of the discrete frequencies, the model accuracy is really high in the middle range of frequencies, but slightly lower for high or low frequencies. An idea to correct this will be to modify the method so that input points can be non equispaced. It will be the target of a future paper.

5 COPYRIGHT STATEMENT

6 ACKNOWLEDGEMENTS

The research leading to these results has received funding from the European Community's Marie Curie Initial Training Network (ITN) on Aircraft Loads Prediction using Enhanced Simulation (ALPES) FP7-PEOPLE-ITN-GA-2013-607911. The partners in the ALPES ITN are the University of Bristol, Siemens and Airbus Operations Ltd.

7 REFERENCES

[1] P. Eykhoff, "System identification parameter and state estimation," 1974.

[2] G. C. Goodwin, D. J. Hill and M. Palaniswami, "A perspective on convergence of adaptive control algorithms," *Automatica,* vol. 20, no. 5, pp. 519-531, 1984.

[3] L. Ljung, "System identification: theory for the user," *PTR Prentice Hall Information and System Sciences Series,* vol. 198, 1987.

[4] K. J. Åström and B. Wittenmark, Adaptive control, Courier Corporation, 2013.

[5] T. Soderstrom and P. Stoica, "System identification," *London : Prentice hall,* vol. 2, 1989.

[6] M. Kern, "Problèmes inverses," *INRIA, Rocquencourt, BP,* vol. 105, p. 78153, 2002.

[7] W. H. Schilders, H. A. Van der Vorst and J. Rommes, Model order reduction: theory, research aspects and applications, vol. 13, Berlin: Springer, 2008.

[8] Å. Björck, "Solving linear least squares problems by Gram-Schmidt orthogonalization," *BIT Numerical Mathematics,* vol. 7, no. 1, pp. 1-21, 1967.

[9] W. E. Arnoldi, "The principle of minimized iterations in the solution of the matrix eigenvalue problem," *Quarterly of Applied Mathematics,* vol. 9, no. 1, pp. 17-29, 1951.

[10] C. Lanczos, "An iteration method for the solution of the eigenvalue problem of linear differential and integral operators," United States Governm. Press Office, 1950.

[11] Y. Shamash, "Stable reduced-order models using Padé-type approximation," *Automatic Control, IEEE Transactions on,* vol. 19, no. 5, pp. 615-616, 1974.

[12] Z. Bai and R. W. Freund, "A partial Padé-via-Lanczos method for reduced-order modeling," *Linear Algebra and its Applications,* vol. 332, pp. 139-164, 2001.

[13] A. C. Antoulas, "An overview of approximation methods for large-scale dynamical systems," *Annual reviews in Control,* vol. 29, no. 2, pp. 181-190, 2005.

[14] A. Odabasioglu, M. Celik and L. T. Pileggi, "PRIMA : Passive reduced-order interconnect macromodeling algorithm," in *Proceedings of the 1997 IEEE/ACM international conference on Computer-aided design,* IEEE Computer Society, 1997, pp. 58-65.

[15] A. C. Antoulas, Approximation of large-scale dynamical systems, Siam, 2005.

[16] B. Moore, "Principal component analysis in linear systems: Controllability, observability, and model reduction," *Automatic control,* vol. 26, no. 1, pp. 17-32, 1981.

[17] A. M. Lyapunov, "The general problem of the stability of motion," *International Journal of Control,* vol. 55, no. 3, pp. 531-534, 1992.

[18] S. Gugercin and A. C. Antoulas, "A survey of model reduction by balanced truncation and some new results," *International Journal of Control,* vol. 77, no. 8, pp. 748-766, 2004.

[19] D. F. Enns, "Model reduction with balanced realizations: An error bound and a frequency weighted generalization.," in *Decision and Control, 1984. The 23rd IEEE Conference on*, IEEE, 1984, pp. 127-132.

[20] G. Wang, V. Sreeram and W. Q. Liu, "A new frequency-weighted balanced truncation method and an error bound," *IEEE Transactions on Automatic Control,* vol. 44, no. 9, pp. 1734-1737, 1999.

[21] P. Feldmann and R. W. Freund, "Efficient linear circuit analysis by Padé approximation via the Lanczos process," *Computer-Aided Design of Integrated Circuits and Systems, IEEE Transactions on,* vol. 14, no. 5, pp. 639-649, 1995.

[22] J.-N. Juang and R. S. Pappa, "An eigensystem realization algorithm for modal parameter identification and model reduction," *Journal of guidance, control, and dynamics,* vol. 8, no. 5, pp. 620-627, 1985.

[23] R. Ober and S. Montgomery-Smith, "Bilinear transformation of infinite-dimensional state-space systems and balanced realizations of nonrational transfer functions," *SIAM Journal on Control and Optimization,* vol. 28, no. 2, pp. 438-465, 1990.

[24] G. H. Golub and C. Reinsch, "Singular value decomposition and least squares solutions," *Numerische Mathematik,* vol. 14, no. 5, pp. 403-420, 1970.

[25] T. McKelvey, H. Akçay and L. Ljung, "Subspace-based multivariable system identification from frequency response data," *Automatic Control, IEEE Transactions on,* vol. 41, no. 7, pp. 960-979, 1996.

[26] U. M. Al-Saggaf and G. F. Franklin, "Model reduction via balanced realizations: an extension and frequency weighting techniques," *Automatic Control, IEEE Transactions on,* vol. 33, no. 7, pp. 687-692, 1988.

[27] D. Schwamborn, T. Gerhold and R. Heinrich, "The DLR TAU-code: Recent applications in research and industry," in *ECCOMAS CFD 2006: Proceedings of the European Conference on Computational Fluid Dynamics, Egmond aan Zee, The Netherlands, September 5-8, 2006*, Delft University of Technology, European Community on Computational Methods in Applied Sciences (ECCOMAS), 2006.

[28] P. R. Spalart and S. R. Allmaras, "A one-equation turbulence model for aerodynamic flows," 1992.

[29] R. H. Landon, "Oscillatory and transient pitching, compendium of unsteady aerodynamic measurements," *AGARD Report No. 702*, 1982.

[30] M. Widhalm, R. P. Dwight, R. Thormann and A. Hübner, "Efficient computation of dynamic stability data with a linearized frequency domain solver," in *European Conference on Computational Fluid Dynamics*, 2010.

[31] A. Da Ronch, A. J. McCracken, K. J. Badcock, M. Widhalm and M. S. Campobasso, "Linear frequency domain and harmonic balance predictions of dynamic derivatives," *Journal of Aircraft,* vol. 50, no. 3, pp. 694-707, 2013.

[32] Z. Bai and R. W. Freund, "A partial Padé-via-Lanczos method for reduced-order modeling," *Linear Algebra and its Applications,* vol. 332, pp. 139-164, 2001.